Revista de la Academia Colombiana de Ciencias Exactas, Físicas y Naturales. 2026
doi: https://doi.org/10.18257/raccefyn.3314

Natural Sciences

Original article

Assessing quinoa's resilience to Martian UV radiation through germination and chlorophyll analysis

Evaluación de la resiliencia de la quinua frente a la radiación UV marciana mediante el análisis de la germinación y la clorofila

Erika Paola Puentes-León[1], Andrea Lizeth López-Rodríguez[1], Zaida Zarely Ojeda-Pérez[2], Santiago Vargas-Domínguez[1,]*

[1] Observatorio Astronómico Nacional, Universidad Nacional de Colombia, Bogotá, Colombia
[2] Grupo de Investigación Bioplasma-UPTC, Facultad de Ciencias, Universidad Pedagógica y Tecnológica de Colombia, Tunja, Colombia

Abstract

As space exploration advances, identifying crops that can withstand extraterrestrial conditions is crucial for establishing sustainable life-support systems. Here, we examined the physiological response of two *Chenopodium quinoa* materials, *Quinoa Real* and *Amarilla de Maranganí,* to simulated Martian ultraviolet (UV) radiation at wavelengths of 180 nm, 250 nm, and 395 nm, compared to a control treatment simulating Earth-like UV (410 nm). Using time-to-event analysis, we found that shorter UV wavelengths (180 nm and 250 nm) significantly accelerated germination, with median germination times nearly three times faster than the control. The Kaplan–Meier and Cox Proportional Hazards models revealed a wavelength-dependent stimulation of germination, with the *Amarilla de Maranganí* variety consistently showing a better performance. Chlorophyll content index measurements further demonstrated that UV exposure, particularly at 180 nm, enhanced chlorophyll accumulation during early seedling development, suggesting an adaptive photoprotective response. These findings underscore quinoa's resilience in germination and early chlorophyll production under UV-induced stress and support its potential as a candidate crop for Martian agriculture. This work contributes to astrobiological efforts aimed at designing robust agricultural systems capable of supporting long-duration human missions beyond Earth.

Keywords: *Chenopodium quinoa*; Extraterrestrial stress tolerance; Ultraviolet wavelength effects; Germination dynamics; Chlorophyll accumulation; Controlled environment agriculture; Astrobiology; Space agriculture.

Resumen

A medida que avanza la exploración espacial, la identificación de cultivos capaces de resistir condiciones extraterrestres resulta crucial para establecer sistemas de soporte vital sostenibles. Se investigó aquí la respuesta fisiológica de dos materiales de *Chenopodium quinoa* — la quinoa real y la amarilla de Maranganí— a radiación ultravioleta (UV) marciana simulada en longitudes de onda de 180 nm, 250 nm y 395 nm, en comparación con un tratamiento control que simulaba la radiación UV terrestre (410 nm). Mediante un análisis de tiempo hasta el evento, se estableció que las longitudes de onda más cortas (180 nm y 250 nm) aceleraron significativamente la germinación, con tiempos medios casi tres veces menores que el control. Los modelos de Kaplan–Meier y de riesgos proporcionales de Cox revelaron una estimulación de la germinación dependiente de la longitud de onda, siendo la variedad amarilla de Maranganí la que mostró consistentemente un desempeño superior. Las mediciones del índice de contenido de clorofila demostraron, además, que la exposición a UV, en particular a 180 nm, incrementó la acumulación de clorofila durante el desarrollo temprano de las plántulas, lo que sugiere una respuesta fotoprotectora adaptativa. Estos hallazgos resaltan la resiliencia de la quinua durante la germinación y la producción temprana de clorofila bajo estrés

Citation: Puentes-León EP, *et al.* Assessing quinoa's resilience to Martian UV radiation through germination and chlorophyll analysis. Revista de la Academia Colombiana de Ciencias Exactas, Físicas y Naturales. 2025 April 29. doi: https://doi.org/10.18257/raccefyn.3314

Editor: Gerhard Fischer

***Corresponding autor:**
Santiago Vargas Dominguez;
svargasd@unal.edu.co

Received: November 18, 2025
Accepted: December 4, 2025
Published on line: April 29, 2026

inducido por radiación UV, lo que respalda su potencial como cultivo candidato para la agricultura marciana. Este trabajo contribuye a los esfuerzos astrobiológicos encaminados al diseño de sistemas agrícolas robustos capaces de sostener misiones humanas de larga duración más allá de la Tierra.

Palabras clave: *Chenopodium quinoa*; Tolerancia a estrés extraterrestre; Efectos de longitudes de onda ultravioleta; Dinámica de germinación; Acumulación de clorofila; Agricultura en ambientes controlados; Astrobiología; Agricultura espacial.

Introduction

As human exploration of Mars becomes an increasingly tangible goal, developing sustainable agricultural systems capable of supporting life beyond Earth has become a critical research priority (**Westall *et al.***, 2013). Mars has an extreme environment, characterized by low atmospheric pressure, frigid temperatures, limited water availability, and intense ultraviolet (UV) radiation due to the absence of a protective ozone layer (**Barth**, 1964; **Owen *et al.***, 1977; **Yamashita *et al.***, 2006; **Hassler *et al.***, 2024). The Martian atmosphere, composed mainly of carbon dioxide, offers minimal shielding against solar UV radiation, particularly in the biologically harmful UV-B and UV-C ranges (200–400 nm) (**Rontó *et al.***, 2006). This high-energy radiation poses a significant challenge to both microbial survival and plant cultivation, necessitating the selection of resilient crops and protective strategies for future extraterrestrial agriculture.

One promising candidate is *Chenopodium quinoa* (quinoa), a highly adaptable Andean crop known for its tolerance to extreme terrestrial environments, including high altitudes, saline soils, drought, and variable radiation levels (**Hussein *et al.***, 2025; **Roman**, 2021; **Cui *et al.***, 2024). Quinoa's physiological resilience suggests that it may also withstand some of the harsh conditions present on Mars, making it an ideal model for investigating plant adaptability in simulated Martian environments.

Previous research has shown that UV exposure can activate stress-responsive mechanisms in plants, such as the production of UV-absorbing compounds and antioxidants, which help mitigate oxidative damage (**Prado *et al.***, 2016; **Salama *et al.***, 2011; **Li *et al.**,* 2022). Exploring whether similar responses occur under Mars-like UV radiation can inform strategies for enhancing crop survival in extraterrestrial settings.

A candidate for Martian agriculture

Chenopodium quinoa is a highly promising candidate for Martian agriculture due to its exceptional adaptability to extreme terrestrial environments. Native to the Andes, quinoa thrives under a wide range of stress conditions, including high UV exposure, low temperatures, saline soils, and drought (**Singh *et al.***, 2019; **Roman**, 2021; **Cui *et al.***, 2024). Its high nutritional value, including a complete amino acid profile, further enhances its suitability for supporting human life in extraterrestrial settings. Previous studies have demonstrated quinoa's ability to activate physiological responses, such as antioxidant production and photoprotective mechanisms, under radiation and biochemical responses to abiotic stressors, including oxidative and hormonal regulation mechanisms that depend on genotype and stress intensity (**Hinojosa *et al.***, 2018; **Shabala *et al.***, 2012). These traits suggest a potential resilience to the harsh environmental conditions present on Mars, where high-energy UV radiation, low atmospheric pressure, and soil nutrient limitations represent critical challenges for plant survival.

Here, we examined the effects of simulated Martian UV radiation on two quinoa materials, *Quinoa Real* and *Amarilla de Marangani*, focusing on germination rates and chlorophyll content as key indicators of stress tolerance and adaptability. By replicating critical aspects of the Martian UV environment, we characterized quinoa's physiological responses to assess its viability as a sustainable food crop for future Mars missions. The findings not only contribute to the growing field of astrobiology but also support the development of robust plant-based life support systems for long-term human exploration and extraterrestrial colonization.

Methods

To place our experimental design in context, we selected UV treatments spanning UV-C (180 nm), UV-B (250 nm), and UV-A (395 nm), plus an Earth-like near-UV control (410 nm). This choice was motivated by the strong wavelength dependence of plant responses to UV radiation and by the growing body of controlled-environment studies showing that UV-B/UVA can induce measurable, dose- and genotype-dependent effects on plant development, photosynthesis-related traits, protective metabolism, and hormonal regulation (**Neugart & Schreiner**, 2018; **Mariotti *et al.***, 2021). Quinoa-specific literature supports this rationale: recent work explicitly examining UV-B stress in quinoa reports significant impacts on germination and early growth, underscoring that quinoa responses are sensitive to UV exposure regime and developmental stage. Additionally, UV-B elicitation experiments in quinoa sprouts/seedlings have demonstrated that short UV-B exposures can modify photosynthetic pigments and phenolic/antioxidant profiles, reinforcing the relevance of pigment-based endpoints in quinoa under UV treatments (**Cardi *et al.***, 2025).

Comparable controlled UV-B supplementation studies in related crop systems provide further methodological precedent: for example, UV-B (and UV-C) treatments have been systematically tested in lettuce cultivars with documented changes in photosynthetic activity and antioxidant properties, and UV-B regimes in amaranth leaves/baby-leaf systems have been explored under defined intensities and exposure durations to elicit stress-protective metabolite responses (**Skowron *et al.***, 2024).

Accordingly, we focused on germination dynamics (time-to-event) as a sensitive integrative metric of early performance under UV exposure, and on chlorophyll status quantified via the chlorophyll content index (CCI) as a rapid, non-destructive proxy for photosynthetic adjustment/acclimation during early seedling development —endpoints widely used in UV-plant physiology and elicitation studies (**Neugart & Schreiner**, 2018).

Experimental setup

To simulate Martian-like UV radiation conditions, a controlled laboratory environment was created with specific UV light sources to replicate the radiation spectrum on Mars (**Cockell *et al.***, 2000). The seeds of each material were sourced from the Germplasm Bank of the Department of Boyacá in Colombia (https://www.gbif.org/es/dataset/0428bf13-3fd0-43cb-b2bd-baec72974ab5), ensuring genetic diversity and suitability for experimental purposes. Two quinoa materials were used in this study: The first corresponded to *Quinoa real* (M1; seed bank code BGQ0009), collected in Ventaquemada (5°22′00.4″N, 73°31′16.9″W) and stored for seven years. The second material was *Amarilla de Maranganí* (M2; BGQ0020), collected in Pasca (4°18′32.8″N, 74°17′59.6″W) and stored for nine years.

The experimental setup consisted of four independent exposure chambers (constructed with a main wooden structure and particleboard panels; an internal lighting system was installed in each chamber, and the interior walls were lined with black cardboard to prevent light leakage and ensure controlled irradiation conditions), each equipped with a UV lamp operating at a nominal peak wavelength of 180 nm, 250 nm, or 395 nm, corresponding respectively to the UV-C, UV-B, and UV-A spectral ranges expected at the Martian surface due to the planet’s thin atmosphere and lack of an ozone layer (**Figure 1S,** https://www.raccefyn.co/index.php/raccefyn/article/view/3314/5324). A fourth chamber served as a control and was equipped with an Earth-like UV-A lamp centered at 410 nm.

Lamp output was initially defined using photometric operating values, with nominal luminous flux settings of 200 lumens (180 nm), 275 lumens (250 nm), 260 lumens (395 nm), and 250 lumens (410 nm, control). These values were used exclusively to ensure stable and repeatable lamp operation and were not interpreted as a measure of ultraviolet irradiance, as lumens are photometric units weighed to the human visual response and are unsuitable for UV quantification, particularly at wavelengths below 400 nm.

To ensure equivalence among exposure chambers, we used lamps of the same make and model within each wavelength category, operated under identical electrical settings. All lamps had comparable usage histories and were allowed to warm up for a fixed period before exposure. Lamps were mounted at a constant distance from the sample surface with perpendicular orientation, and all Petri dishes were placed within the uniformly illuminated region of each chamber, fully covered by the lamp footprint and free of shading or obstructions (**Table 1S,** https://www.raccefyn.co/index.php/raccefyn/article/view/3314/5324).

Direct radiometric measurements of irradiance at the seed surface (mW cm^{-2}) were not available for this experimental campaign. To ensure reproducibility, therefore, we provide a complete description of the UV sources and exposure geometry. Lamps were operated at manufacturer-specified electrical power, and exposure duration, lamp-to-sample distance, illuminated area, and chamber geometry were kept identical across all treatments, ensuring that differences between experimental conditions reflect spectral effects rather than geometric or temporal variability. Detailed information on lamp make and model, nominal peak wavelengths, full spectral emission distributions, electrical power ratings, manufacturer-provided radiant flux (when available), and lamp-to-sample geometry is provided in **Table 1S,** https://www.raccefyn.co/index.php/raccefyn/article/view/3314/5324, to allow independent reconstruction or estimation of irradiance in future studies.

Throughout the experiment, environmental parameters, including temperature and humidity, were continuously monitored to ensure uniform conditions across all experimental chambers. Temperature and relative humidity were constantly monitored using calibrated digital sensors. Environmental conditions were maintained at 14.1 °C and 72% relative humidity, with fluctuations remaining within ±0.5 °C and ±3% RH throughout the experiment. All exposure chambers were operated under identical environmental conditions for the full duration of the study, also ensuring that any observed effects on germination and chlorophyll production could be attributed solely to the UV radiation treatments. Each chamber contained 12 Petri dishes with quinoa seeds. Twenty seeds were placed in each dish, totaling 240 seeds per treatment. This setup ensured consistent exposure to the simulated Martian UV radiation, allowing for detailed observations on the effects of varying wavelengths and intensities on seed germination and chlorophyll production.

Biological material

The biological material used consisted of two quinoa materials, *Quinoa Real* (labeled M1) and *Amarilla de Maranganí* (labeled M2), chosen for their nutritional value and potential adaptability to extreme environmental conditions. *Quinoa real*, a high-altitude variety traditionally grown in the Andean region, is known for its resilience to low temperatures and high UV exposure. *Amarilla de maranganí*, a variety also cultivated in high-altitude areas, possesses notable tolerance to various environmental stressors, making both materials suitable candidates for testing under simulated Martian conditions.

Before the experiment, the seeds underwent a standardized preparation process. Each batch was initially cleaned and sorted to remove any damaged or undersized seeds. To ensure uniformity, seeds were then under controlled conditions (14.1 °C and 72% relative humidity) until we started the experiment, minimizing any pre-exposure to stress.

For the experimental trials, 20 seeds of each variety were placed in individual Petri dishes, twelve per UV treatment and control condition, resulting in 12 independent biological replicates per treatment and per quinoa material (240 seeds per material per treatment). Each Petri dish was lined with moistened filter paper to provide a stable moisture source, and seeds were evenly spaced to prevent overlap and ensure uniform exposure to the simulated Martian UV radiation.

The Petri dish was defined as the experimental unit for all germination analyses to avoid pseudoreplication. At the start of the experiment, Petri dishes were randomly assigned to positions within each exposure chamber and placed within the uniformly illuminated region. Chamber geometry and lamp configuration were identical across treatments, minimizing potential plate and position effects during UV exposure.

Figure 1 illustrates representative visual examples of *Chenopodium quinoa* seed samples obtained during different stages of the experiment, highlighting at first glance the morphological responses under ultraviolet radiation exposure. Panels (a) and (b) correspond to the *Amarilla de Maranganí* material. In (a), seeds are shown at the initial stage of the experiment, before UV treatment, with intact seed coats and no visible germination. Panel (b) shows the same material after the completion of the germination assay, where most seeds have initiated radicle emergence, indicating successful germination. Panels (c) and (d) display the germination response of *Quinoa Real* seeds after UV exposure. In these Petri dishes, seeds exhibit clear signs of physiological activity, with radicle and hypocotyl elongation. Panels (e), (f), and (g) offer close-up views of *Amarilla de maranganí* seeds during different stages of the germination process. Image (e) captures the very early phase of radicle emergence, (f) shows the development of the embryonic axis with increased chlorophyll pigmentation, and (g) presents a fully germinated seedling with a clearly extended radicle. These images provide morphological evidence of quinoa’s capacity to progress through the key stages of early plant development under simulated Martian UV conditions. The details of the quantitative analysis will be addressed in the following sections.

Measurement techniques

To assess the impact of simulated Martian UV radiation on the physiological and biochemical properties of *C. quinoa*, we used a series of standardized measurement techniques. These methods were designed to evaluate key indicators of plant stress and adaptation, including germination rates and chlorophyll content. By leveraging precise observational protocols and custom Python-based analysis scripts implementing Kaplan–Meier estimators and Cox proportional hazards models, the study aimed to ensure accurate and reproducible results.

Germination rates

To evaluate the effects of simulated Martian UV radiation on quinoa seed germination, germination rates were measured for both *Quinoa Real* and *Amarilla de Maranganí* materials under each UV treatment and the control condition. Germination was defined as

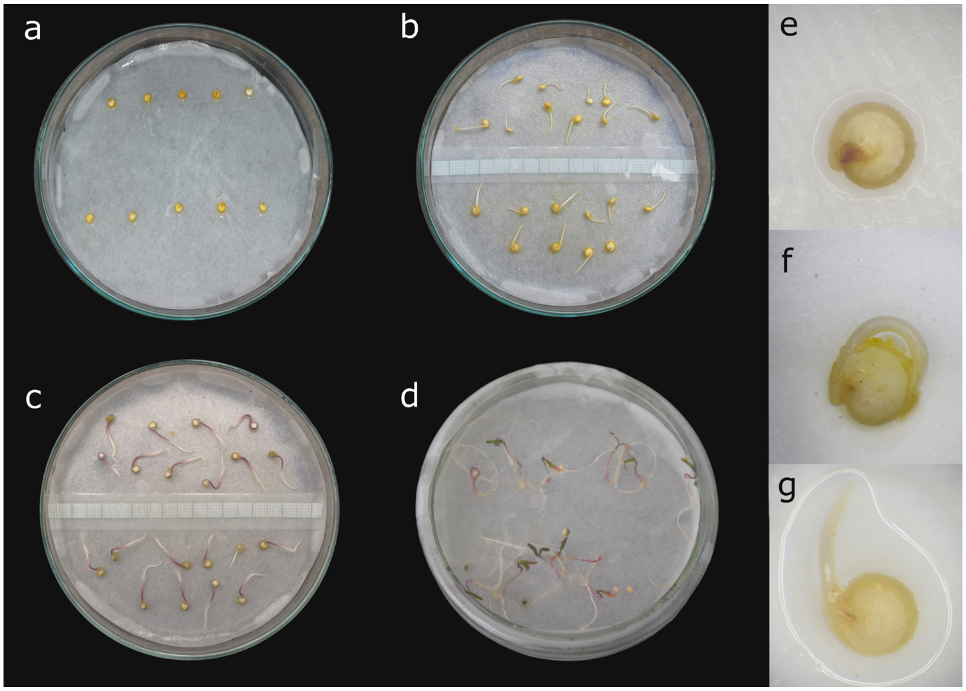

Figure 1. Representative images of *Chenopodium quinoa* seed germination under experimental conditions. **(a)** *Amarilla de Maranganí* seeds before UV exposure. **(b)** Same variety after germination. **(c–d)** *Quinoa Real* after UV-induced germination. **(e–g)** Close-up views of different germination stages in *Amarilla de Maranganí*, showing radicle emergence **(e)**, hypocotyl development **(f)**, and early seedling formation **(g)**

the visible emergence of the radicle (root tip) from the seed coat, and seeds were considered germinated only when the radicle reached a minimum length of 1 mm, ensuring consistent identification of successful germination events.

Germination was monitored over an 84-hour period at fixed observation intervals (every 2 hours), during which all Petri dishes were systematically inspected. At each time point, the number of seeds meeting the germination criterion was recorded. Scoring was performed by the same trained observer following a standardized protocol, using an objective morphological criterion to minimize observer bias.

At the end of the 84-hour observation period, the final germination rate was calculated as the percentage of germinated seeds relative to the total number of seeds per dish. Seeds that did not meet the germination criterion by 84 h were retained in the dataset and treated as right-censored observations in subsequent time-to-event (survival) analyses.

Kaplan–Meier estimator

The Kaplan–Meier estimator is a non-parametric statistic widely used to estimate the survival function of time-to-event data (**Kaplan & Meier**, 1958). Here, we adapted this method to analyze germination data by treating the emergence of the radicle as the “event” of interest. This approach allowed us to account for variability in germination times across different UV treatments and provided a robust means to compare germination dynamics between the two quinoa materials, M1 and M2, under simulated Martian UV radiation.

For each treatment group, we recorded the time (in hours) at which each seed germinated, considering germination successful when the radicle length reached at least 1 mm. Seeds that failed to germinate during the 84-hour observation period were treated as censored data, as their germination status remained unknown beyond the study’s duration. The Kaplan–Meier estimator was calculated using the formula:

$$S(t) = \prod_{t_i \leq t} (1 - d_i/n_i),$$

where $S(t)$ is the estimated survival function at time t, d_i is the number of seeds germinated at time t_i, and n_i is the number of seeds at risk of germinating at time t_i. This formula allowed us to estimate the probability of seeds having not germinated by a given time point. The Kaplan–Meier survival curves for each treatment group were plotted, and statistical comparisons between groups were conducted using the log-rank test. This test assessed whether differences in germination dynamics across various UV wavelengths (180 nm, 250 nm, 395 nm, and 410 nm) were statistically significant. Additionally, confidence intervals for the survival estimates were calculated to provide a measure of uncertainty in the data.

Chlorophyll content

Chlorophyll content was used as an indicator of photosynthetic status and physiological response to simulated Martian UV radiation in one-month-old M1 and M2 seedlings. The plants were placed in bags containing soil, rice husk, and peat, and these same plants were used during the experimental stage. Measurements were performed at regular intervals during and after UV exposure to track stress-induced changes and early acclimation responses.

The CCI was quantified using a portable chlorophyll meter (Apogee MC-100, Apogee Instruments Inc., Logan, USA), which provides non-destructive estimates of relative chlorophyll levels. CCI measurements were conducted on the same cohort of seedlings repeatedly over time, using the first fully expanded true leaf when available or the cotyledons at earlier developmental stages.

For each seedling, three technical readings per leaf were taken at each time point, and the average value was used for analysis. Individual seedlings were treated as the biological units to avoid pseudoreplication. Measurements were recorded every five hours over a 75-hour monitoring period following the onset of UV exposure. Before each measurement session, the instrument was checked and calibrated according to the manufacturer’s recommendations, and instrument settings were kept constant throughout the experiment.

Results and analysis

To assess the effects of simulated Martian irradiance on quinoa seed germination, we conducted experiments exposing seeds to three Martian-like UV wavelengths (180 nm, 250 nm, and 395 nm) and compared their performance to a control group subjected to Earth-like UV radiation (410 nm).

Germination dynamics were analyzed using time-to-event methods to account for differences in germination timing among treatments. Kaplan–Meier survival curves were constructed for each UV treatment and quinoa material, and differences between curves were assessed using Cox proportional hazards models.

The proportional hazards assumption of the Cox models was evaluated using Schoenfeld residuals, including both statistical tests and visual inspection of residual plots. Additional graphical diagnostics, such as the inspection of Kaplan–Meier curves, were used to identify potential violations of proportionality.

Seeds that did not germinate by the end of the 84-hour observation period were treated as right-censored observations. No interpolation of germination times was performed; all analyses were based on observations recorded at discrete time points.

Table 1 summarizes the germination parameters of seeds under different wavelengths, while **Figure 2** provides a detailed depiction of germination dynamics under UV exposure. The left panel shows the number of newly germinated seeds recorded at

Table 1. Germination parameters of *Quinoa real* (M1) and *Amarilla de Maranganí* (M2) seeds under different wavelengths. Each group consists of 80 seeds.

Wavelength (nm)	Parameter	M1 Group 1	M1 Group 2	M1 Group 3	M2 Group 1	M2 Group 2	M2 Group 3
180 nm	Germination time for the highest seed quantity (h)	12	12	13	13	13	13
180 nm	Quantity of germinated seeds	60	42	42	52	50	75
180 nm	Germinated seeds (%)	75	52.5	52.5	65	63	94
250 nm	Germination time for the highest seed quantity (h)	14	9	15	13	13	13
250 nm	Quantity of germinated seeds	56	34	44	78	73	76
250 nm	Germinated seeds (%)	70	43	55	98	91	95
395 nm	Germination time for the highest seed quantity (h)	16	35	35	15	15	16
395 nm	Quantity of germinated seeds	37	48	44	73	80	90
395 nm	Germinated seeds (%)	16	48	55	91	86	72
410 nm (Control)	Germination time for the highest seed quantity (h)	37	29	30	28	29	28
410 nm (Control)	Quantity of germinated seeds	24	80	23	52	29	38

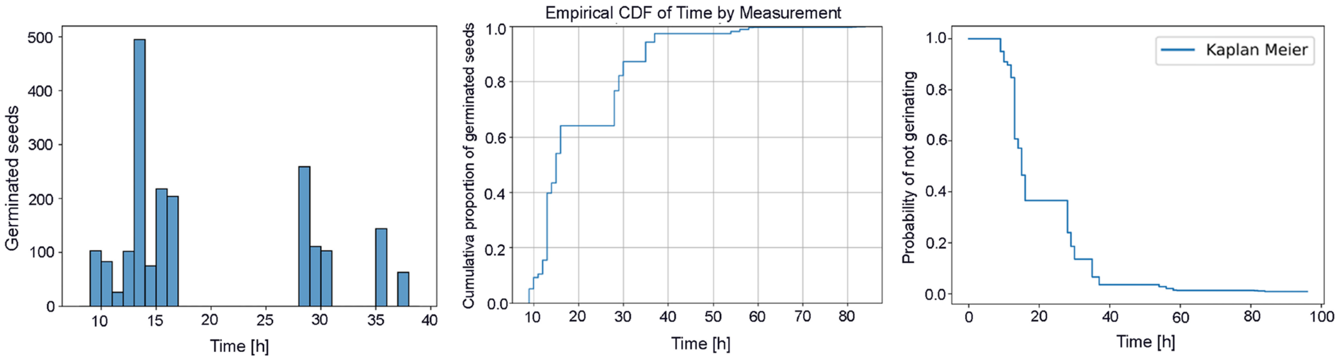

Figure 2. *Left*: Numbers of newly germinated seeds recorded at each observation interval, representing seeds that germinated between consecutive assessments. *Center*: The same data plotted as cumulative totals. *Right*: Kaplan-Meier curve of probability of not germinating. Median survival time 15.0 h

discrete observation time points. Due to logistical constraints, no observations were recorded during an intermediate time window, resulting in a temporary gap in the time series. The central panel presents the cumulative proportion of germinated seeds based on the available observation points. Germination progressed rapidly during the initial phase, followed by a latency interval corresponding to the observation gap, and then resumed at later time points.

The right panel shows the Kaplan–Meier survival curve, representing the probability of seeds remaining ungerminated over time. The curve exhibits a steep initial decline associated with early germination events, followed by a period of apparent stabilization reflecting the absence of observations, and a subsequent decline as additional germination events were recorded. The median survival time, defined as the time at which 50% of seeds had germinated, was 15 hours, indicating that most germination occurred early in the experiment.

To quantify the relative risk of germination over time, we applied the Cox Proportional Hazards model (**Cox**, 1972), which assumes that the hazard ratio between groups remains constant (time-invariant) and that each treatment modifies the baseline hazard by a multiplicative factor. The survival curves presented in **Figure 3** indicate that both quinoa materials exhibit faster germination under shorter UV wavelengths (180 nm and 250 nm), as reflected by the steeper decline in the probability of not germinating. At 180 nm, variety M2 shows consistently higher germination hazard than M1, whereas at 250 nm, both varieties display similar survival trajectories. Under longer wavelengths (395 nm and 410 nm), germination is delayed and more variable, particularly for M1. Overall, these patterns confirm a clear wavelength-dependent effect of UV radiation on germination dynamics, with M2 exhibiting a higher probability of early germination across treatments. Differences among treatments were statistically significant (log-rank test, $p < 0.05$). All analyses were performed using Python. These findings underscore the wavelength-dependent influence of UV radiation on quinoa seed germination and highlight the importance of integrating time-to-event analyses in studies of plant responses to abiotic stressors, particularly in the context of astrobiological research.

Seed germination analysis

The germination performance of the two quinoa materials showed distinct responses to UV treatments. M2 consistently exhibited higher germination rates compared to M1, particularly under shorter UV wavelengths (180 nm and 250 nm). This suggests a greater adaptability of *Amarilla de Maranganí* to UV-induced stress, which may be attributed to genetic or physiological factors. **Table 2** summarizes the germination parameters for both materials under each treatment. Seeds exposed to 180 nm UV radiation germinated

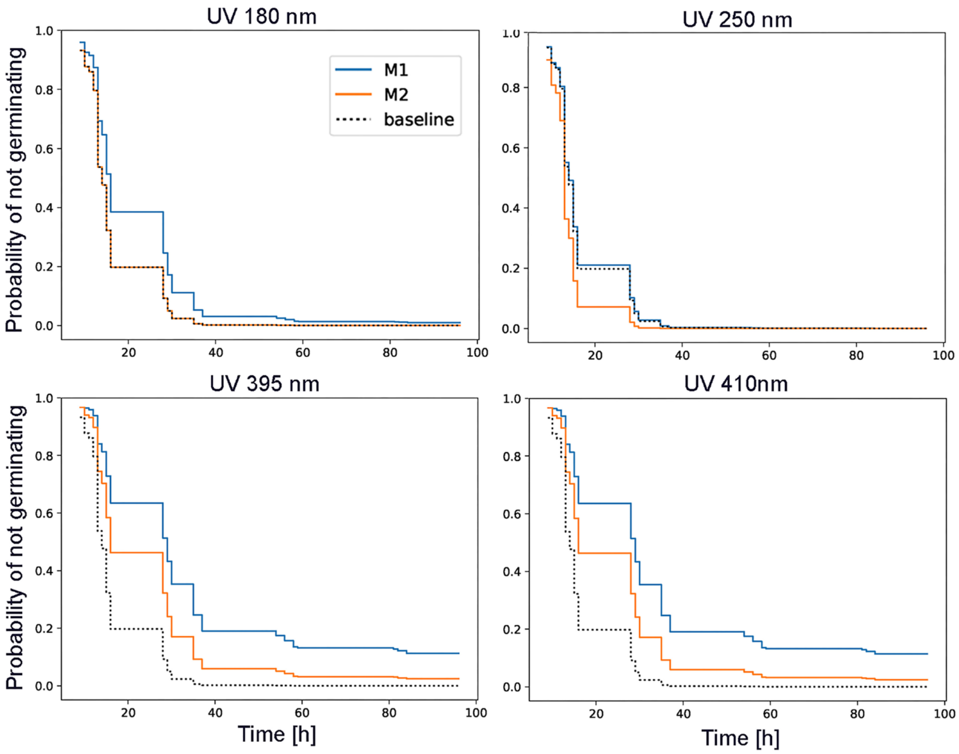

Figure 3. Probability of no germination showing the dynamics for *Chenopodium quinoa* seeds under different UV irradiance levels for *Quinoa Real* (M1) and *Amarilla de Marangani* (M2), as labeled

Table 2. Summary of germination parameters for *Quinoa Real* (M1) and *Amarilla de Marangani* (M2) under different UV treatments

Wavelength (nm)	Variety	Mean Germination Time (h)	Germination Rate (%)	Peak Germination Time (h)
180	M2	12	74	12
180	M1	14	75	13
250	M2	13	95	13
250	M1	15	70	14
395	M2	16	72	15
395	M1	35	55	16
400 (control)	M2	28	38	28
400 (control)	M1	30	23	30

significantly faster, with a mean germination time of 12 hours for M2, compared to 14 hours for M1. The control group displayed the slowest germination rates, with mean times exceeding 30 hours for both materials.

Figure 4 shows the cumulative germination curves of seeds exposed to different UV wavelengths for M1 and M2. Differences in germination dynamics are observed depending on the wavelength and seed type. For example, at 395 nm and 410 nm, seeds associated with M2 exhibit faster and more synchronized germination compared to M1. At 250 nm, both seed types showed rapid and nearly simultaneous germination. These results highlight the influence of UV wavelength and seed type on germination timing and rate.

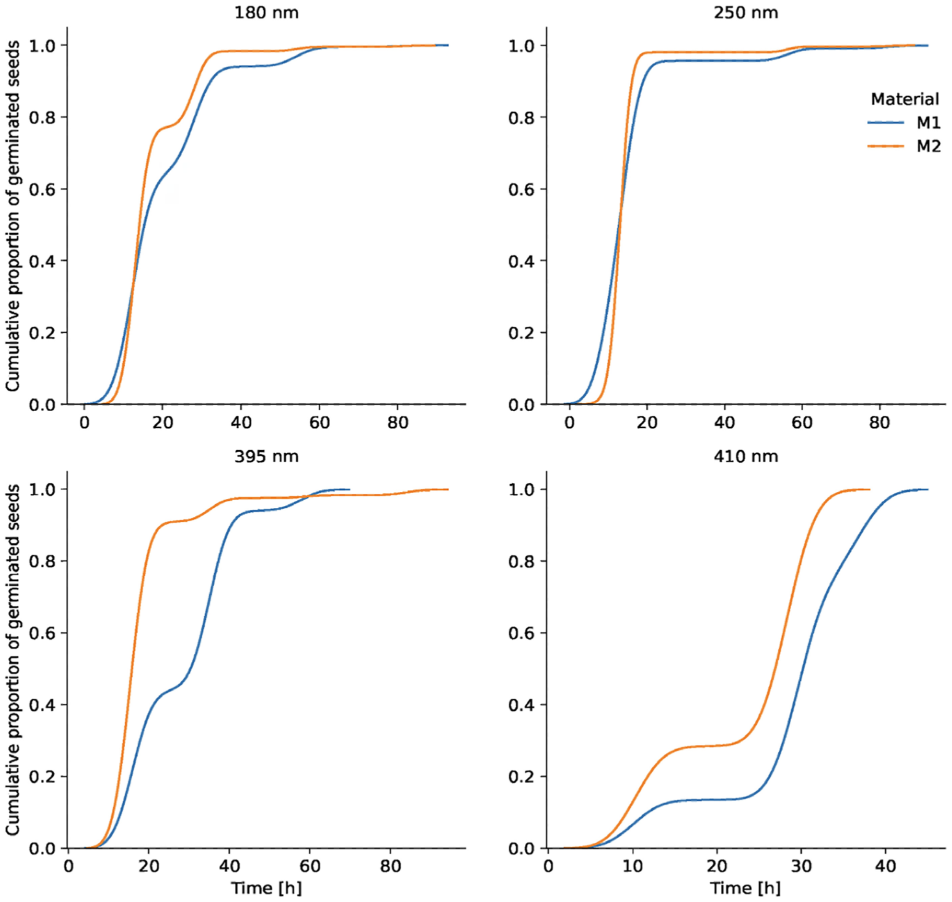

Figure 4. Smoothed cumulative germination curves of seeds exposed to different UV wavelengths (180 nm, 250 nm, 395 nm, and 410 nm) for *Quinoa Real* (M1) and *Amarilla de Maranganí* (M2), as labeled. The plots show the cumulative proportion of germinated seeds over time (in hours). Differences in germination dynamics are observed depending on the wavelength and seed type (M1 or M2).

Figure 5 displays the cumulative germination curves showing the proportion of all germinated seeds over time under different UV wavelengths. Each curve represents the smoothed response across various wavelengths. Germination was fastest and most synchronized under 250 nm, while delays and plateaus are more evident at longer wavelengths (395 nm and 410 nm), especially at 410 nm, where a marked lag phase appears between 17 and 27 hours. These results suggest that UV wavelength significantly influences the timing and rate of seed germination.

Chlorophyll levels

The chlorophyll content index (CCI) was monitored over time to assess the photosynthetic response of quinoa seedlings to UV radiation at 180 nm. **Figure 6** shows the temporal evolution of CCI for both materials, M1 (left) and M2 (right), together with their respective Gaussian fits. In contrast to the previous section, the CCI time-series analysis incorporates a more comprehensive statistical treatment, allowing a clearer identification of the temporal dynamics and amplitude of the physiological response. In both cases, CCI exhibits an initial slight decrease during the early exposure period, followed by a pronounced rise that peaks between approximately 39 and 41 hours. This delayed maximum indicates a non-immediate photosynthetic adjustment, likely linked to the activation of protective or repair pathways within the photosynthetic machinery. After the peak, CCI values gradually

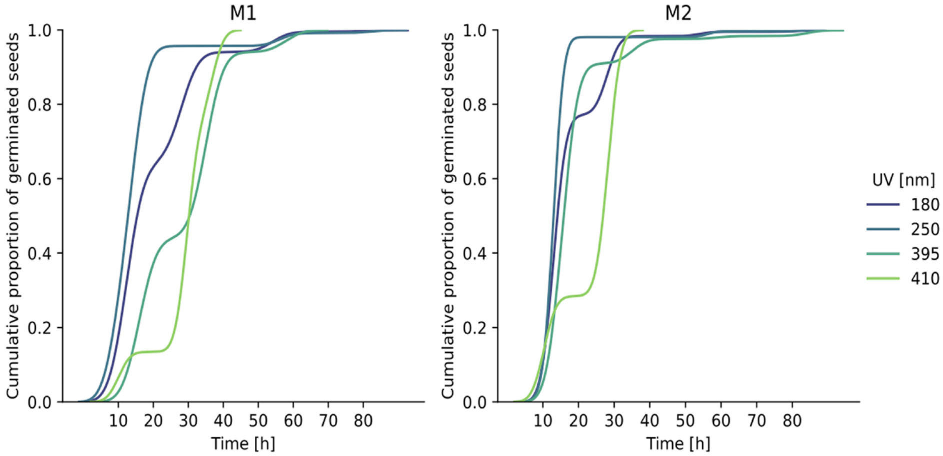

Figure 5. Smoothed cumulative germination curves showing the proportion of germinated seeds over time under different UV wavelengths (180 nm, 250 nm, 395 nm, and 410 nm, in colors). *Left*: *Quinoa Real* (M1) and *Right*: *Amarilla de Maranganí* (M2)

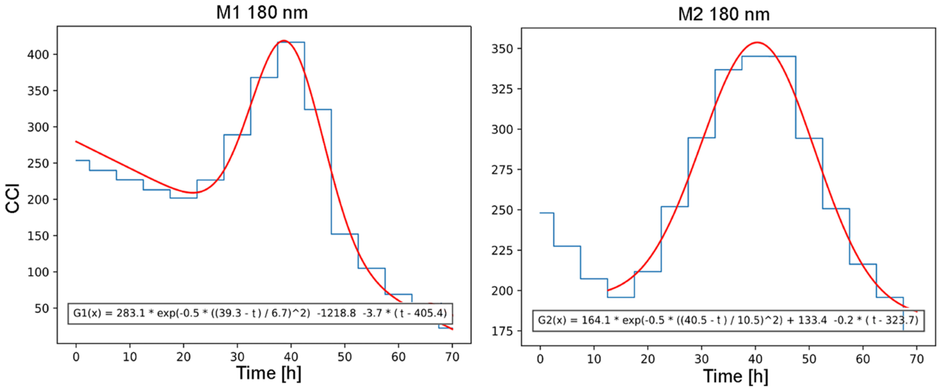

Figure 6. *Blue*: Measured chlorophyll content index (CCI) over time for *Quinoa Real* (left: M1) and *Amarilla de Maranganí* (right: M2) under UV radiation of 180 nm. *Red*: The fitted curve according to the Gaussian formulas at the bottom

decline, suggesting either the onset of photoinhibition or a stabilization phase following acclimation to the stress conditions. Quantitatively, M1 reaches a higher CCI peak (~410) compared with M2 (~350), revealing a stronger compensatory photosynthetic response in this material under UV stress. The fitted Gaussian models captured this single dominant response phase with high fidelity, highlighting that the chlorophyll synthesis did not follow a sustained or multi-phase pattern.

It is important to note, however, that gaps in the dataset—particularly in the central portion of the measurement series (as also seen in **Figure 1S,** https://www.raccefyn.co/index.php/raccefyn/article/view/3314/5324)— required smoothing and curve fitting to describe the overall temporal trend. Consequently, inferences drawn from these intervals carry significant uncertainty, and the exact timing and magnitude of intermediate fluctuations should be interpreted with caution. Despite this limitation, the general trends and fitted curves provide a consistent framework for understanding the delayed yet pronounced chlorophyll response to extreme UV exposure.

Figure 7 presents the temporal evolution of chlorophyll content index (CCI) for the two quinoa materials (M1, magenta; M2, cyan) under three UV treatments (180 nm, 250

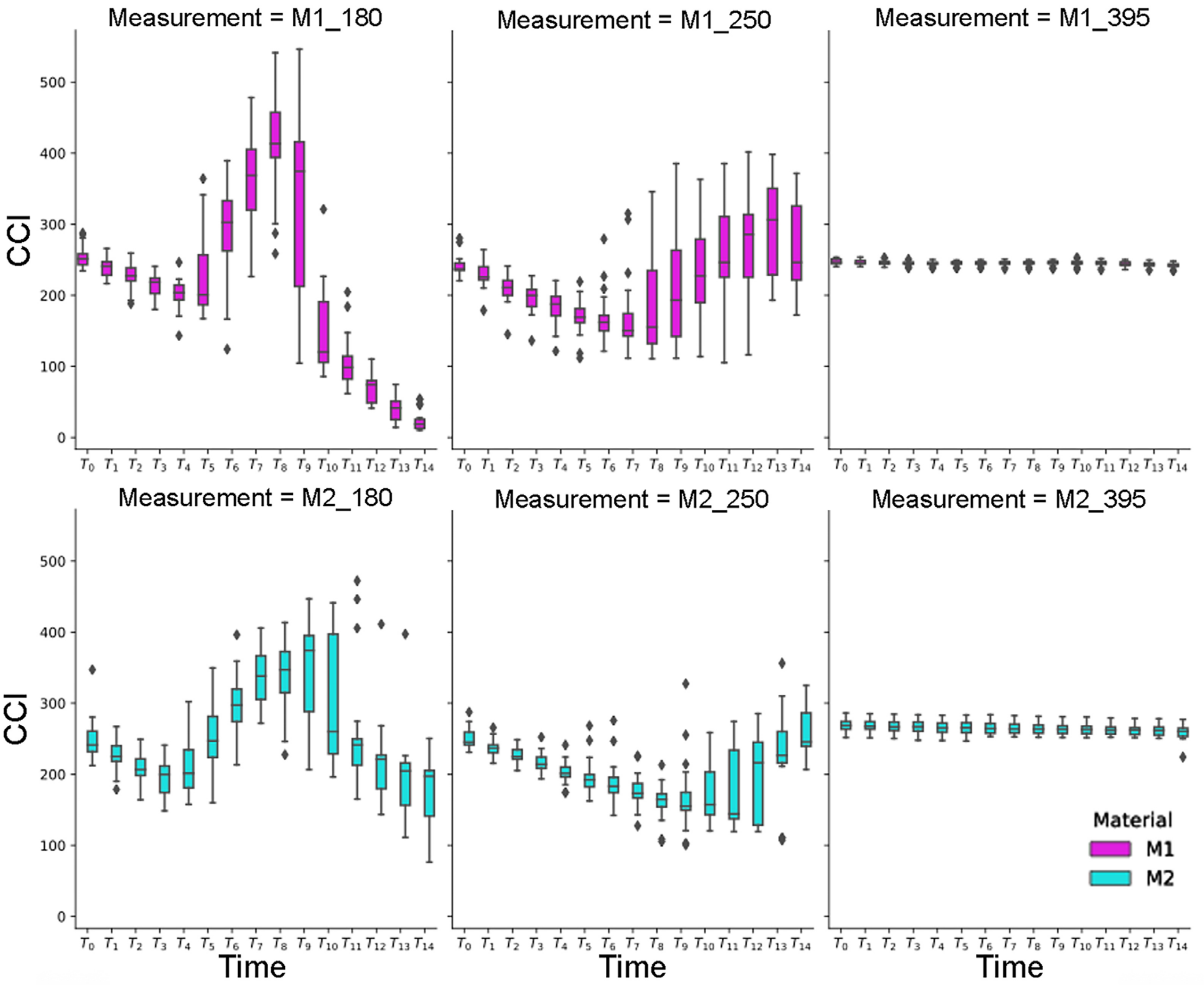

Figure 7. Temporal evolution of the Chlorophyll Content Index (CCI) for two quinoa materials (*Quinoa Real*, M1 in magenta; *Amarilla de Maranganí*, M2 in cyan) under three ultraviolet radiation treatments: 180 nm, 250 nm, and 395 nm. Each subplot displays boxplots representing the distribution of CCI values across 15 time points (T0–T14).

nm, 395 nm). Responses are strongly wavelength- and time-dependent, and fluctuations in the CCI are indicators of increased stress in the plants. Under 180 nm irradiation, both materials exhibit a pronounced, transient response. This is, CCI falls modestly in the earliest time points, then rises sharply to a distinct peak in the mid-experiment interval (approximately T6–T8) before declining rapidly toward the final time points. This mid-experiment peak is larger and more variable for M1 than for M2, indicating a greater amplitude (and inter-individual variability) of the short-wavelength response in M1. Note that at 180 nm, the stress response appears early and is particularly pronounced. Under 250 nm irradiation, the pattern is different. In this case, both materials show a modest early decline in CCI followed by a gradual recovery and increasing CCI at later time points (T8–T14); variability also increases toward the end of the series. By contrast, the 395 nm treatment shows essentially no temporal change in CCI for either variety (tight, near-constant boxplots across times from T0 to T14).

Taken together, the boxplots indicate that short-wavelength UV (180 nm) produced a strong, transient alteration in chlorophyll status (larger in M1), 250 nm produced a delayed recovery after an early depression, and 395 nm produced a negligible change.

Discussion and conclusions

Results interpretation

Our results are consistent with the growing body of literature on plant adaptive responses to ultraviolet (UV) radiation, particularly regarding the mechanisms that enable quinoa to withstand and even benefit from shortwave UV-A and UV-B exposure. The observed acceleration of germination and the increase in chlorophyll content under simulated Martian UV conditions indicate that *C. quinoa* activates a set of photomorphogenic and antioxidant pathways that mitigate radiation-induced stress while promoting early development.

At the physiological level, the responses observed in quinoa are consistent with the activation of UV-responsive signaling pathways, including the UVR8–COP1–HY5 cascade, which mediates UV perception and regulates the expression of genes involved in photomorphogenesis, antioxidant defense, and the synthesis of UV-screening compounds, such as flavonoids and anthocyanins (**Jansen *et al.***, 1998; **Jenkins**, 2014; **Tilbrook *et al.***, 2013; **Robson *et al.***, 2015). It is important to note that the chlorophyll content index (CCI) is not a direct output of this signaling pathway, but rather a functional proxy reflecting the balance between photosynthetic capacity, stress-induced damage, and subsequent acclimation. Therefore, the observed CCI dynamics likely integrate multiple downstream processes, including oxidative stress responses, pigment turnover, and repair mechanisms, rather than direct transcriptional regulation by UVR8 signaling alone.

Although UVR8-mediated signaling is known to induce flavonoid and anthocyanin accumulation, these pigments were not quantified in the present study, and no systematic assessment of visible pigment intensity was performed. Future work combining chlorophyll measurements with targeted pigment profiling would be required to disentangle the relative contributions of photosynthetic pigments and UV-screening compounds to the responses observed.

The transient nature of the chlorophyll content response, with an initial decline followed by a pronounced peak, suggests a sequence of early oxidative stress followed by acclimation and repair, consistent with the generation and controlled detoxification of reactive oxygen species (ROS) through enzymes, such as superoxide dismutase (SOD), catalase (CAT), and ascorbate peroxidase (APX) (**Hideg *et al.***, 2013).

The accelerated germination rates recorded under 180–250 nm exposures can be interpreted within a hormetic framework, where moderate UV doses act as positive stressors that trigger physiological reprogramming. Previous studies have shown that UV exposure can alter the balance of phytohormones, such as gibberellins, auxins, and abscisic acid, leading to increased seed coat permeability and faster radicle emergence (**Prado *et al.***, 2016; **Hussein *et al.***, 2025; **Robson *et al.***, 2015). This hormetic stimulation of germination observed in quinoa is like the behavior reported in other stress-tolerant crops, such as amaranth and barley, where UV exposure promotes synchronized germination and early vigor under moderate stress conditions (**Neugart & Schreiner**, 2018).

The varietal differences observed between *Quinoa Real* (M1) and *Amarilla de Maranganí* (M2) further emphasize the role of genetic diversity in adaptive plasticity. *Amarilla de Maranganí* exhibited higher germination rates and more stable chlorophyll dynamics, consistent with previous reports indicating that certain Andean landraces possess enhanced tolerance to UV, salinity, and drought due to higher basal levels of flavonoids, phenolics, and osmoprotectants (**Bazile *et al.***, 2015; **Prado *et al.***, 2016). This differential response may reflect genotype-dependent differences in early UV signaling and in protective metabolites present in the seed coat and emerging tissues, although these compounds were not quantified in this study. The higher chlorophyll peak observed in *Quinoa Real*, in contrast, suggests a stronger compensatory photosynthetic adjustment that may entail greater metabolic cost.

From a photosynthetic perspective, the delayed chlorophyll peak (~39–41 h) under shortwave UV exposure likely reflects a late physiological adjustment following initial stress. Given the limited amount of photosynthetic tissue at this stage and the absence of direct measurements of photosystem II performance or repair mechanisms, mechanistic interpretations such as D1 protein turnover remain speculative. Nevertheless, this pattern is consistent with general UV-induced acclimation responses reported in the literature (**Jenkins**, 2014; **Natarajan *et al.***, 2024).

Implications for Martian agriculture

Mars has severe constraints for plant growth, including intense UV radiation, extreme temperatures, and low atmospheric pressure, which limit gas exchange and photosynthetic performance. While our results show that quinoa can tolerate UV stress through accelerated germination and chlorophyll-related responses, these findings reflect adaptation to a single stress factor under Earth conditions. Therefore, quinoa should be regarded as a candidate for further studies in controlled, partially pressurized greenhouse systems. Moreover, the increased chlorophyll content observed under UV exposure may provide an additional advantage for photosynthetic efficiency in low-light conditions, a scenario frequently encountered in Martian greenhouses. Such conditions are expected due to the lower solar irradiance at Mars compared to Earth, the strong attenuation of incoming light during atmospheric dust events, and the use of protective or partially shielded greenhouse structures designed to mitigate radiation exposure, all of which can substantially limit the photosynthetically active radiation reaching the crops.

These findings suggest that controlled UV exposure could be incorporated into Martian agricultural systems to stimulate beneficial adaptive responses in crops, reducing reliance on Earth-like conditions that are resource-intensive to replicate. In this context, quinoa's capacity to convert UV-induced oxidative stress into metabolic stimulation makes it an ideal candidate for experimental validation in extraterrestrial agriculture systems, complementing recent work on crop viability in Martian regolith and controlled photobioreactor systems (**Eichler *et al.***, 2021; **Poulet *et al.***, 2022).

Limitations and future directions

While this study provides promising insights into quinoa's adaptability under simulated Martian UV radiation, several limitations must be addressed to fully assess its potential for extraterrestrial agriculture. The experiments were conducted in controlled laboratory settings that, although simulating some Martian environmental factors, do not capture the complexity of the planet's surface. Key aspects such as low gravity, Martian soil composition, and long-term exposure to harsh conditions were not included in this study and could significantly influence plant performance.

Future research should extend the duration of UV exposure to investigate its long-term impacts on plant growth, yield, and reproduction. Exploring the effects on chlorophyll dynamics and the genetic and biochemical pathways driving stress responses will provide deeper insights into quinoa's resilience. Additionally, experiments in Mars analog environments, such as the Mars Desert Research Station (MDRS) (**Poulet *et al.***, 2014), the Hawaii Space Exploration Analog and Simulation (HI-SEAS) (**Binsted**, 2016), the Concordia Station (**Durante**, 2017), the Mars Society's Flashline Mars Arctic Research Station (**Bishop**, 2004), and the Habitat Análogo de Exploración Espacial Simulada en Colombia (HAdEES) (**Botero**, 2023), could validate laboratory findings and offer practical knowledge for implementing agricultural systems on Mars.

Expanding the scope of research to include other stress-tolerant crops, such as amaranth or legumes, will help diversify the pool of potential Martian crops, ensuring greater food security and adaptability. Advances in genetic engineering may also play a crucial role in enhancing quinoa's resilience, tailoring its traits to meet the specific demands of extraterrestrial agriculture. By continuing to investigate stress-tolerant crops like quinoa and integrating advanced methodologies, we can make significant progress toward establishing sustainable agricultural systems that support human life beyond Earth. This research will not only aid in developing Martian agricultural systems but also contribute valuable knowledge to agricultural practices in extreme environments on Earth.

Supplementary information

See the supplementary information in https://www.raccefyn.co/index.php/raccefyn/article/view/3314/5324

Acknowledgements

The research was sponsored by the DynaSun project and has thus received funding under the Horizon Europe programme of the European Union under grant agreement No. 101131534. The views and opinions expressed are, however, those of the authors and do not necessarily reflect those of the European Union, which cannot, therefore, be held responsible for them. Acknowledgments are also extended to the team of collaborators from the Bioplasma research group at the Pedagogical and Technological University of Colombia (UPTC), who assisted in data collection during the experimental process.

Author contributions

EPPL conceived the research question, collected and interpreted the data, and contributed to the writing and revision of the manuscript; **ALLR** assisted with data collection, performed the statistical analyses, and participated in the writing and revision of the manuscript; **ZZOP** and **SVD** contributed to defining the research question, conducted the literature review, carried out the analysis and discussion, and drafted the manuscript.

Conflicts of interest

The authors declare that they have no conflicts of interest.

References

Barth, C. A. (1974). The atmosphere of Mars. *Annual Review of Earth and Planetary Sciences, 2*, 333-367.

Bazile, D., Bertero, H. D., Nieto, C. (Eds.). (2015). *State of the Art Report on Quinoa around the World in 2013.* FAO & CIRAD.

K. A. Binsted, M. Basner, W. Bedwell, B. Caldwell, D. Chang, J. Hunter, S. Kozlowski, J. Nasrini, P. Roma, J. Santoro, M. Seibert, B. Shiro, P. Wu (2016). Investigations at hi-seas into team function and performance on long duration exploration missions. In *NASA 2016 Human Research Program Investigators’ Workshop*, Galveston, Texas, USA.

Bishop, S. L. (2004). Evaluating teams in extreme environments: From issues to answers. *Aviation, space, and environmental medicine, 75,* C14-21.

Botero-Botero, M. A. (2023). *Diseño de un hábitat análogo de bajo costo en Colombia: Hábitat Análogo de Exploración Espacial Simulada Colombia, HAdEES-C* [Trabajo de grado en Ingeniería Aeroespacial, Universidad de Antioquia]. https://hdl.handle.net/10495/36971

Carli, M., Guglielminetti, L., Huarancca Reyes, T. (2025). UVB Stress Induced Changes in Germination and Carbohydrate Mobilization in *Chenopodium Quinoa* Willd. Seeds. *Seeds*, *4*(3), 46. https://doi.org/10.3390/seeds4030046

Clark, B. C. (1998). Surviving the limits to life at the surface of Mars. *Journal of Geophysical Research: Planets, 103*(E12), 28545-28555.

Cockell, C. S., Catling, D. C., Davis, W. L., Snook, K., Kepner, R. L., Lee, P., McKay, C. P. (2000). The ultraviolet environment of Mars: Biological implications past, present, and future. *Icarus, 146*(2), 343-359.

Cox, D. R. (1972). Regression models and life-tables (with discussion). *Journal of the Royal Statistical Society: Series B (Methodological), 34*(2), 187-220.

Cui, H., Yao, Q., Xing, B., Zhou, B., Shah, S. S., Qin, P. (2024). The performance of agronomic and quality traits of quinoa under different altitudes in Northwest of China. *Agronomy, 14*(6), 1194.

Durante, M., Dartnell, L., Kausch, C., Narici, L., McKenna-Lawlor, S., Sihver, L., Sabatier, L., Reitz, G., Weber, U. (2017). Recommendations for ESA-supported ground-based research on space radiation protection. *ESA Topical Team IBER, Nordwijk, the Netherlands*.

Eichler, A., Hadland, N., Pickett, D., Masaitis, D., Handy, D., Pérez, A., Batcheldor, D., Wheeler, B., Palmer, A. (2021). Challenging the agricultural viability of Martian regolith simulants. *Icarus, 354*, 114022.

Hassler, D. M., Zeitlin, C., Wimmer-Schweingruber, R. F., Ehresmann, B., Rafkin, S., Eigenbrode, J. L., Brinza, D. E., Weigle, G., Böttcher, S., Böhm, E., Burmeister, S., Guo, J., Köhler, J., Martin, C., Reitz, G., Cucinotta, F. A., Kim, M.-H., Grinspoon, D., Bullock, M. A., … Moores, J. E. (2014). Mars' surface radiation environment measured with the Mars Science Laboratory's Curiosity rover. *Science, 343*(6169), 1244797. https://doi.org/10.1126/science.1244797

Hideg, É., Jansen, M. A. K., Strid, Å. (2013). UV-B exposure, ROS, and stress: Inseparable companions or loosely linked associates? *Trends in Plant Science, 18*(2), 107-115.

Hinojosa, L., González, J. A., Barrios-Masias, F. H., Fuentes, F., Murphy, K. M. (2018). Quinoa Abiotic Stress Responses: A Review. *Plants*, *7*(4), 106. https://doi.org/10.3390/plants7040106

Hussein, F. A., Basuny, A. M., Farghaly, H. E., Abou-Zaid, F. O. F. (2025). Quinoa (Chenopodium Quinoa Willd.) is a highly nutritious source of grains. *World Scientific Research*, *12*(1), 46-53.

Jansen, M. A. K., Gaba, V., Greenberg, B. M. (1998). Higher plants and UV-B radiation: balancing damage, repair and acclimation. *Trends in Plant Science*, *3*, 131-135.

Jenkins, G.I. The UV-B photoreceptor UVR8: From structure to physiology. *Plant Cell, 26*(1), 21-37.

Kaplan, E. L. & Meier, P. (1958). Nonparametric estimation from incomplete observations. *Journal of the American Statistical Association, 53*(282), 457-481. https://doi.org/10.1080/01621459.1958.10501452

Li, C., Zhang, X., Ye, T., Li, X., Wang, G. (2022). Protection and damage repair mechanisms contributed to the survival of *Chroococcidiopsis* sp. exposed to a Mars-like near space environment. *Microbiology Spectrum, 10*(6), e03440-22.

Mariotti, L., Huarancca Reyes, T., Ramos-Diaz, J. M., Jouppila, K., Guglielminetti, L. (2021). Hormonal Regulation in Different Varieties of *Chenopodium quinoa* Willd. Exposed to Short Acute UV-B Irradiation. *Plants*, *10*(5), 858. https://doi.org/10.3390/plants10050858

Natarajan, S., Vinoth Kumar, R., Subbiah, M., Selvaraj, I. R., Pillathil Senthil Mani, P. J., Murugan, S., Allasamy, P. (2024). Plant responses to UV-B radiation. *African Journal of Biological Sciences, 6*(8), 2238-2256.

Neugart, S. & Schreiner, M. (2018). UVB and UVA as eustressors in horticultural and agricultural crops. *Scientia Horticulturae, 234*, 370-381.

Owen, T., Biemann, K., Rushneck, D. R., Biller, J. E., Howarth, D. W., Lafleur, A. L. (1977). The composition of the atmosphere at the surface of Mars. *Journal of Geophysical Research, 82*(28), 4635-4639.

Patel, M. R., Zarnecki, J. C., Catling, D. C. (2002). Ultraviolet radiation on the surface of Mars and the Beagle 2 UV sensor. *Planetary and Space Science, 50*(9), 915-927. https://doi.org/10.1016/S0032-0633(02)00079-2

Poulet, L., Engeling, K., Hatch, T., Stahl-Rommel, S., Vélez-Justiniano, Y-A., Castro-Wallace, S., Bunchek, J., Monje, O., Hummerick, M., Khodadad, C.L.M., Spencer, L.E., Pechous, J., Johnson, C.M., Fritsche, R., Massa, G.D., Romeyn, M.W., O'Rourke, A.E., Wheeler, R.W. (2022) Large-Scale Crop Production for the Moon and Mars: Current Gaps and Future Perspectives. Frontiers in astronomy and space sciences, *8*, 733944. https://doi.org/10.3389/fspas.2021.733944

Poulet, L. & Doule, O. Greenhouse automation, illumination and expansion study for Mars Desert Research Station. In *Proceedings of the IAC 2014* (Toronto, ON, Canada, September 29-October 3, 2014).

Prado, F. E, Pérez, M. L, González, J. A. (2016). Efectos de la radiación ultravioleta B (UV-B) sobre diferentes variedades de Quinoa: II.- efectos sobre la síntesis de pigmentos fotosintéticos, protectores y azúcares solubles en condiciones controladas. *Boletín de la Sociedad Argentina de Botánica*, *51*(4), 665-673.

Robson, T. M., Klem, K., Urban, O., Jansen, M. A. (2015). Re-interpreting plant morphological responses to UV-B radiation. *Plant, Cell & Environment, 38*(5), 856-866.x

Rontó, G., Bérces, A., Lammer, H., Cockell, C. S., Molina-Cuberos, G. J., Patel, M. R., Selsis, F. (2003). Solar UV irradiation conditions on the surface of Mars. *Photochemistry and Photobiology, 77*(1), 34-40.

Roman, V. J. (2021). *Salt tolerance strategies of the ancient Andean crop quinoa* [Tesis doctoral, Wageningen University and Research].

Salama, H. M., Al Watban, A. A., Al-Fughom, A. T. (2011). Effect of ultraviolet radiation on chlorophyll, carotenoid, protein and proline contents of some annual desert plants. *Saudi Journal of Biological Sciences, 18*(2), 125-129.

Shabala, L., Mackay, A., Tian, Y., Jacobsen, S. E., Zhou, D., Shabala, S. (2012). Oxidative stress protection and stomatal patterning as components of salinity tolerance mechanism in quinoa (*Chenopodium quinoa*). *Physiologia Plantarum, 146*(1), 26-38. https://doi.org/10.1111/j.1399-3054.2012.01599.x

Singh, D. (2019). Quinoa (*Chenopodium quinoa* Willd). Scientific Publishers.

Tarasashvili, M. V., Sabashvili, S. A., Tsereteli, S. L., Aleksidze, N. G. (2013). New model of Mars surface irradiation for the climate simulation chamber 'Artificial Mars'. *International Journal of Astrobiology, 12*(2), 161-170.

Skowron, E., Trojak, M., Pacak, I. (2024). Effects of UV-B and UV-C Spectrum Supplementation on the Antioxidant Properties and Photosynthetic Activity of Lettuce Cultivars. *International Journal of Molecular Sciences*, *25*(17), 9298. https://doi.org/10.3390/ijms25179298

Tilbrook, K., Arongaus, A. B., Binkert, M., Heijde, M., Yin, R., Ulm, R. (2013). The UVR8 UV-B photoreceptor: Perception, signaling and response. *The Arabidopsis Book, 11*, e0164.

Vicente-Retortillo, A., Valero, F., Vázquez, L., Martínez, G. M. (2015). A model to calculate solar radiation fluxes on the Martian surface. *Journal of Space Weather and Space Climate, 5*, A33. https://doi.org/10.1051/swsc/2015035

Westall, F., Loizeau, D., Foucher, F., Bost, N., Bertrand, M., Vago, J., Kminek, G. (2013). Habitability on Mars from a microbial point of view. *Astrobiology, 13*(9), 887-897.

Yamashita, M., Ishikawa, Y., Kitaya, Y., Goto, E., Arai, M., Hashimoto, H., Tomita-Yokotani, K., Hirafuji, M., Omori, K., Shiraishi, A., Tani, A., Toki, K., Yokota, H., Fujita, O. (2006). An overview of challenges in modeling heat and mass transfer for living on Mars. *Annals of the New York Academy of Sciences, 1077*, 232-243. https://doi.org/10.1196/annals.1362.012